0026-895X/00/010002-11$3.00/0
Copyright © The American Society for Pharmacology and Experimental Therapeutics
All rights of reproduction in any form reserved.
MOLECULAR PHARMACOLOGY, **57:**2–12 (2000).

Reduced Apoptosis after Nerve Growth Factor and Serum Withdrawal: Conversion of Tetrameric Glyceraldehyde-3-Phosphate Dehydrogenase to a Dimer

GRAEME W. CARLILE, RUTH M. E. CHALMERS-REDMAN, NADINE A. TATTON, AMANDA PONG, KATHERINE E. BORDEN, and WILLIAM G. TATTON

Departments of Neurology (G.W.C., R.M.E.C.-R., N.A.T., A.P., K.L.B.B., W.G.T.) and Physiology and Biophysics (K.L.B.B.), Mount Sinai School of Medicine, New York, New York

Received August 5, 1999; accepted September 20, 1999

This paper is available online at http://www.molpharm.org

ABSTRACT

Antisense oligonucleotides against the glycolytic enzyme glyceraldehyde-3-phosphate dehydrogenase (GAPDH) are able to reduce some forms of apoptosis. In those forms, overall GAPDH levels increase and the enzyme accumulates in the nucleus. The monoamine oxidase B (MAO-B) inhibitor, (−)-deprenyl (DEP), its metabolite (−)-desmethyldeprenyl, and a tricyclic DEP analog, CGP3466, can reduce apoptosis independently of MAO-B inhibition and have been found to bind to GAPDH. We used neuronally differentiated PC12 cells to show that DEP, DES, and CGP3466 reduce apoptosis caused by serum and nerve growth factor withdrawal over the concentration range of 10^{-} to 10^{-13} M. We provide evidence that the DEP-like compounds bind to GAPDH in the PC12 cells and that they prevent both the apoptotic increases in GAPDH levels and nuclear accumulation of GAPDH. In vitro, the compounds enhanced the conversion of NAD^{+} to NADH by GAPDH in the presence of AUUUA-rich RNA and converted GAPDH from its usual tetrameric form to a dimeric form. Using cell lysates, we found a marked increase in rates of NAD^{+} to NADH conversion in early apoptosis, which was returned toward control values by the DEP-like compounds. Accordingly, the DEP-like compounds appear to decrease glycolysis by preventing the GAPDH increases in early apoptosis. GAPDH dimer may not have the capacity to contribute to apoptosis in a similar manner to the tetramer, which might account for the antiapoptotic capacity of the compounds. These actions on GAPDH, rather than MAO-B inhibition, may contribute to the improvements in Parkinson's and Huntington's diseases found with DEP treatment.

Studies with antisense oligonucleotides showed that glyceraldehyde-3-phosphate dehydrogenase (GAPDH) is necessary for apoptosis to proceed in cerebrocortical neurons and PC12 cells (Ishitani et al., 1996; Sawa et al., 1997). GAPDH levels increase during the early part of apoptosis (Sunaga et al., 1995; Ishitani et al., 1996, 1997, 1998; Saunders et al., 1997). In nonapoptotic cells, GAPDH is primarily found in the extra nuclear cytoplasm with only sparse localization to small punctate areas in the nucleus (Carlile et al., 1998). In apoptosis, GAPDH accumulates densely in the nucleus, and that accumulation has been proposed to underlie its role in apoptosis (Saunders et al., 1997; Sawa et al., 1997; Ishitani et al., 1998; Shashidharan et al., 1999).

GAPDH may participate in the pathogenesis of some neurodegenerative diseases. GAPDH binds to the mutant proteins with polyglutamine repeats in Huntington's disease (HD) and related degenerative conditions (Burke et al., 1996). GAPDH is found in amyloid plaques in Alzheimer's disease (AD) brains (Sunaga et al., 1995), and GAPDH nuclear accumulation is present in association with apoptosis in nigral neuronal nuclei in postmortem Parkinson's disease (PD) brain (N. Tatton, unpublished observations). Although there is evidence for metabolic abnormalities in HD tissues, GAPDH glycolytic activity does not appear to be altered in HD brain tissue (Kish et al., 1998).

Neuronal loss, likely by apoptosis, is central to AD, HD, and PD (Cotman, 1998; Tatton et al., 1998; Petersen et al., 1999). The monoamine oxidase B (MAO-B) inhibitor (−)-deprenyl (DEP) slows the progression of PD clinical deficits (Parkinson's Study Group, 1993; Olanow et al., 1995) and

The work was supported by a Lowenstein Foundation Grant and Medical Research Council of Canada Grants (to W.G.T. and K.L.B.B.).

ABBREVIATIONS: GAPDH, glyceraldehyde-3-phosphate dehydrogenase; DEP, (−)-deprenyl; DES, (−)-desmethyldeprenyl; PML, promyelocytic leukemia; BL, BODIPY-labeled; PND, partially neuronally differentiated; LCSM, laser confocal scanning microscopy; M/S+N, minimum essential medium with serum and nerve growth factor; BCA, bicinchoninic acid; NGF, nerve growth factor; M/O, minimum essential medium only; CGP3466, *N*-methyl-*N*-propargyl-10^{-}aminomethyl-dibenzo[*b*,*f*]oxepin; HD, Huntington's disease; AD, Alzheimer's disease; PD, Parkinson's disease; MAO-B, monoamine oxidase B.

may also reduce clinical deficits in HD (Patel et al., 1996). The basis for clinical improvements with DEP are uncertain because the clinical trial data do not allow for the differentiation of a slowed rate of neuronal loss from a symptomatic effect like that caused by increased dopamine availability (see Fahn, 1996). DEP and its metabolite, (−)-desmethyldeprenyl (DES), reduce apoptosis in a variety of cells (Tatton et al., 1994; Le et al., 1997; Paterson et al., 1997, 1998; Kragten et al., 1998; Magyar et al., 1998; Maruyama et al., 1998; Wadia et al., 1998) via mechanisms that are independent of MAO-B inhibition (Tatton and Chalmers-Redman, 1996) and require new protein synthesis (Tatton et al., 1994). CGP3466, a tricyclic DEP analog (*N*-methyl-*N*-propargyl-10-aminomethyl-dibenzo[*b*,*f*]oxepin), which does not have the capacity to inhibit MAO-B, reduces apoptosis and binds specifically to GAPDH (Kragten et al., 1998). The GAPDH binding has been proposed to account for the antiapoptotic capacities of DEP-like compounds.

We have carried out experiments in vivo and in vitro to determine whether DES and CGP3466 reduce apoptosis caused by serum and NGF withdrawal in a similar manner to DEP (Tatton et al., 1994; Wadia et al., 1998) and whether any reduction in apoptosis by DES and CGP3466 can be linked to actions on GAPDH.

Materials and Methods

PC12 cells were propagated in minimum essential medium (MEM) containing 10% horse serum and 5% fetal bovine serum. The cells were transferred to 24-well plates and partially neuronally differentiated (PND) for 6 days in the same media supplemented with 100 ng/ml 7S nerve growth factor [NGF; MEM with serum and NGF (M/S+N); see Wadia et al. (1998) for details of culture, treatment, preparation, staining, and counting]. On day 6, the cells were washed repeatedly to remove NGF and serum-borne trophic agents and replaced in M/S+N as controls, in MEM only (M/O) for trophic withdrawal, or in MEM with DEP, DES, or CGP3466 at concentrations varying from 10^{-5} to 10^{-13} M. At 24 h after washing, cells were harvested and lysed, and intact nuclei were counted as an estimate of cell survival (Fig. 1A, filled circles).

The cells were also grown and treated as above on poly(L-lysine)-treated coverglass and were stained with YOYO-1 (Molecular Probes, Eugene, OR) at various times after washing to reveal chromatin condensation as a marker of apoptotic nuclear degradation (see Wadia et al., 1998, for references). Cells on coverglass were washed three times in PBS and then put in 100% methanol at −20°C

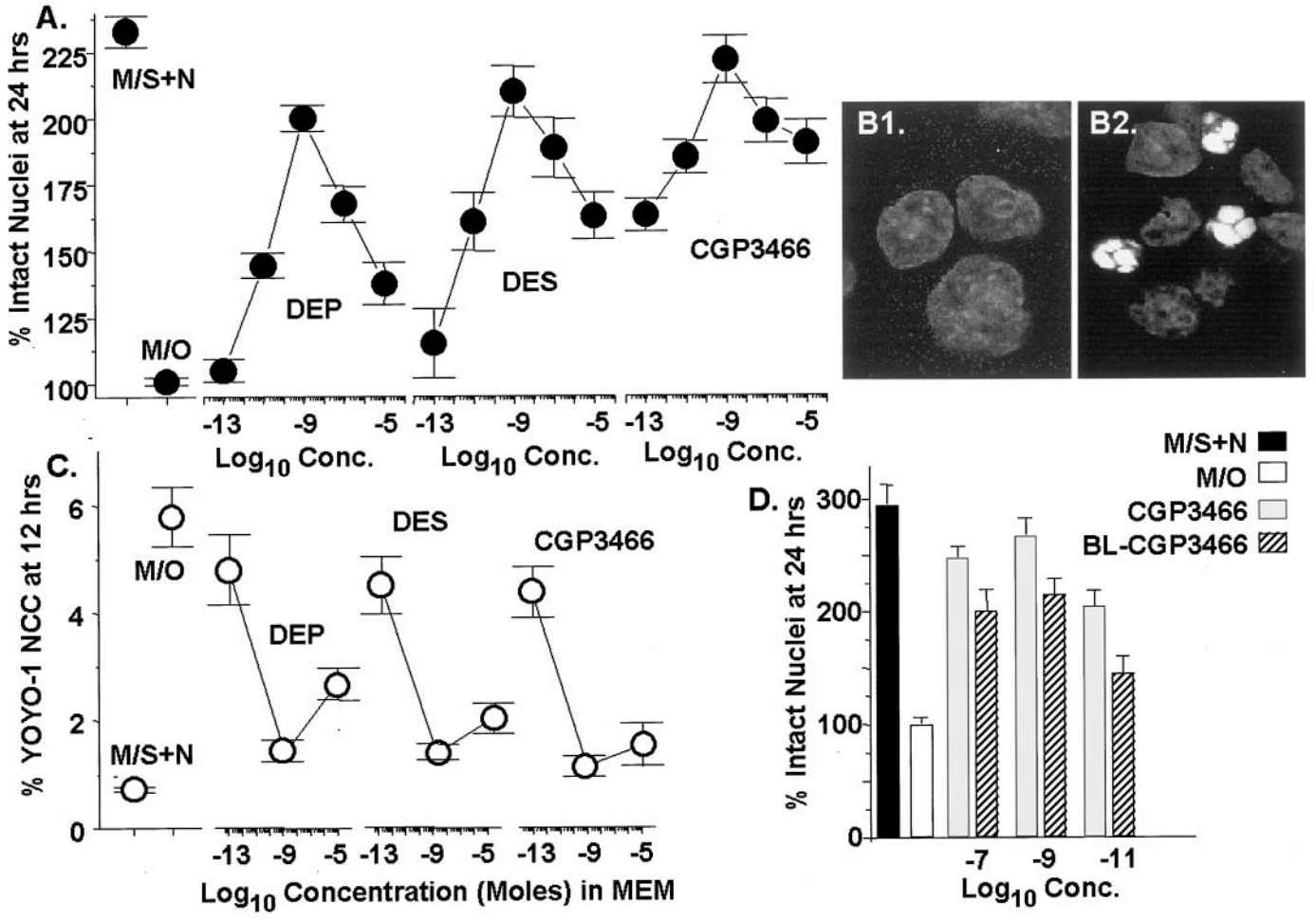

Fig. 1. DEP-related compounds reduce apoptosis. DEP, DES, and CGP3466 at concentrations ranging between 10^{-13} and 10^{-5} M increase the survival of PND-PC12 cells as estimated by numbers of intact nuclei (A) and decrease the number of nuclei with apoptotic nuclear degradation as shown by nuclear chromatin condensation revealed by YOYO-1 DNA staining at the same concentrations (C). M/S+N indicates cells that were washed repeatedly to remove trophic support and then replaced in MEM with serum and NGF. M/O indicates cells that were washed and then placed in MEM only. B1 and B2, typical examples of YOYO-1 stained normal nuclei and nuclei with chromatin condensation, respectively. D, comparison of the numbers of intact nuclei for cells treated with CGP3466 and those treated with BL-CGP3466 showing that the BL compound retains most of the capacity of the unlabeled compound to reduce cell death.

for 30 s. The cells on coverglass were then incubated in 1.5 μM YOYO-1 in PBS at room temperature for 30 min. The cells were then washed three times in PBS and mounted in Aquamount (Gurr, England). The total number of YOYO-1 stained nuclei were counted on 25 fields for each coverslip, each field was chosen by the use of pairs of randomly generated *x-y* coordinates, and the number of nuclei with chromatin condensation were expressed as a percentage. The values were pooled for three coverslips for each treatment and time point.

Laser confocal scanning microscopic (LCSM) images were collected using a Leica TCS4D confocal microscope equipped with a tunable excitation filter. Images were collected with a 100× 1.4 NA objective at a pinhole setting of 20 to minimize focal depth. Images were collected in a 512 × 512 × 8 bit format and saved as TIFF files. Images of live cells exposed to BODIPY-labeled (BL)-CGP3466 or DES were similarly acquired using an environmentally controlled chamber (Medical Systems Corp.) that houses a 25-mm coverglass on which PC12 cells were plated and treated as above. YOYO-1 was imaged using excitation/emission values of 488 nm/515 to 545 nm, whereas BODIPY-FL images and GAPDH immunoreaction fluorescence were taken at 568/585 to 615 and 647/660 long pass, respectively.

To identify the proteins that bind CGP3466 in the PND PC12 cells, cells were incubated with ^{125}I photoaffinity-labeled CGP3466 at varying times after serum and NGF withdrawal. After exposure to ultraviolet light, total protein was extracted, run on gels, and transferred to a membrane. PC-12 cells were grown in MEM with serum and NGF for 6 days, and then serum and NGF were withdrawn. One hour before harvesting, 6 μCi of the photoaffinity-labeled CGP3466 was added. Thirty minutes later, the dishes were put in a UV transilluminator for 20 min to activate the azido group. After removal of the medium and one wash with balanced salt solution, the cells were harvested using trypsin-EDTA and then centrifuged at 1000*g* for 5 min. The supernatant was removed and the cells were washed twice in PBS. The cells were lysed in lysis buffer (25 mM Tris · HCl, pH 7.5, 150 mM NaCl, 1 mM EDTA, and 1% Triton X-100), and the samples were stored frozen at −20°C. Samples were run on an SDS-polyacrylamide gel and transferred to a nitrocellulose membrane. The membrane was dried and exposed on x-ray film. After completion of the autoradiographic exposure, the same membranes were probed for GAPDH immunoreactivity using a mouse monoclonal antibody (Chemicon International, Temecula, CA) at a dilution of 1:400.

For determinations of the time course of changes in GAPDH levels, cells were grown on 10-cm Petri dishes for 6 days and treated as above. At 0.5 to 12 h after washing, cells were harvested, and a lysate was produced. The medium was removed and placed in a separate tube on ice, and 2 ml of PBS was added to each dish. The cells were removed with a cell scraper and centrifuged for 5 min at 1500*g* at 4°C, followed by cold PBS washes. The cells were then centrifuged at 2000*g* and lysed in lysis buffer (25 mM Tris · HCl, pH 7.5, 150 mM NaCl, 1 mM EDTA, 1% Triton X-100, and 5 μg/ml leupeptin, chymostatin, pepstatin A, and aprotinin, plus 1 mM benzamidine). The lysate was stored at −30°C. Protein was assayed by the bicinchoninic acid (BCA) method.

To obtain protein from various subcellular fractions, the cells were treated as above and harvested by centrifugation at 1000*g* for 5 min at 4°C. The pellets were washed twice in cold PBS and resuspended buffer containing 25 mM HEPES-KOH, pH 7.5,10 mM KCl, 1.5 mM $MgCl_2$, 1 mM NaEDTA, 1 mM NaEGTA, 1 mM dithiothreitol, and 5 μg/ml leupeptin, chymostatin, pepstatin A, and aprotinin, plus 1 mM benzamidine and 250 mM sucrose. The cells were homogenized by 12 to 15 strokes of a glass Dounce homogenizer. The homogenates were then centrifuged at 700*g* for 10 min at 4°C. This pellet is the nuclear fraction, and the supernatants was further centrifuged at 10,000*g* for 15 min at 4°C. The resulting pellet represents the mitochondrially enriched fraction, and the supernatant represents the cytoplasmic fraction. Both nuclearly and mitochondrially enriched fractions were resuspended in 50 μl of the above buffer. Samples were then frozen at −30°C. Before use, the samples were protein assayed by the BCA method. Equal amounts of whole-cell or subcellular fraction lysates were run on a SDS-polyacrylamide gel, Western blotted, and probed for GAPDH as above.

To demonstrate the enrichment of cellular subfractions, equal amounts of protein from each fraction were Western blotted and probed with antibodies for nucleolin (1:500; Santa Cruz Biochemicals, Santa Cruz, CA), 14-3-3 β protein (1:400; Santa Cruz Biochemicals), and cytochrome oxidase (0.1 μg/ml; Molecular Probes, Eugene, OR), which are markers for the nuclear, cytoplasmic, and mitochondrial fractions, respectively.

For immunocytochemistry and the examination of the kinetics of cellular entry and accumulation of fluorescently labeled DES and CGP3466, PC-12 cells were grown on a coverglass and partially neuronally differentiated as described (for details, see Tatton et al., 1994; Wadia et al., 1998). Cells were fixed in 4% paraformaldehyde and then washed once in PBS and placed in 5% normal goat serum and 0.01% Tween-20 in PBS for 1 h at room temperature. The cell on coverglass were again washed with PBS; placed in a solution containing 0.5% normal serum, 0.01% Tween-20, and mouse monoclonal GAPDH antibody at a 1:300 dilution; and incubated overnight at 4°C. The cells on a coverglass were washed four times with PBS and exposed to a Cy5-labeled goat anti-mouse secondary antibody (Jackson Immunoresearch, West Grove, PA) at a dilution of 1:500 in PBS containing 0.5% normal serum and 0.01% Tween-20 for 1 h at room temperature. The cells on coverglass were washed five times in PBS and mounted in Aquamount.

Three-dimensional protein structural models of rat GAPDH were produced as in Borden (1998) and are described here briefly. The structure of rat GAPDH has not been reported. GAPDH structures were obtained from the Brookhaven protein database. GAPDH is highly conserved in terms of its amino acid sequence and three-dimensional structure (Kim et al., 1995). After inspection of structures of GAPDH from several species, we decided to use a GAPDH from *Leishmania mexicana*, in which the structure had been determined under physiological salt conditions, although this structure did not look significantly different from any other GAPDH structures in the database (Kim et al., 1995). Using the program Insight (Biosym, San Diego, CA), we modeled the rat GAPDH sequence onto the *L. mexicana* structure. The subsequent structure was subjected to molecular dynamics at 1000 K, followed by cooling to 300 K, and then underwent 1000 steps of conjugate gradient minimization using Discover (Biosym).

The glycolytic activity of GAPDH, measured by the increase in absorption at 340 nm, resulting from the reduction of NAD^+ to NADH according to the reaction glyceraldehyde-3-phosphate + NAD^+ + P_i = 1,3-diphosphoglycerate + NADH. The enzyme assay was carried out in the presence of 0.015 M sodium pyrophosphate, pH 8.5, 7.5 mM NAD^+, 0.1 M dithiothreitol, and 0.015 M GAPDH. Immediately before its use, the enzyme was diluted in the pyrophosphate buffer to a concentration of 30 μg/ml. A synthetic RNA oligonucleotide of 15 residues consisting of three repeating AUUUA sequences (Genosys, Ltd., Cambridge, UK) was used in the glycolytic studies. The glycolytic activity of cell lysates produced from a 6-h exposure to MS+N, M/O, and MO+DES was similarly determined. Cells were collected in 0.015 M sodium pyrophosphate buffer, pH 8.5, and homogenized with a Dounce homogenizer; protein was assayed by the BCA method (Pierce Chemical, Rockford, IL) and stored at −20°C. Equal amounts of total protein were incubated in 0.015 M sodium pyrophosphate, pH 8.5, with NAD^+ and dithiothreitol, and the conversion of NAD+ to NADH was determined as above.

To examine the oligomeric states of GAPDH, Sephacryl H-300 was poured into a glass column to a height of 12 cm and diameter of 1 cm. The column was washed using a buffer containing 20 mM HEPES, pH 7.5, 25 mM KCl, and 10% glycerol. Samples were loaded onto the column in volumes of less than 100 μl. Samples including more than one component were coincubated briefly before addition to the column. GAPDH, CGP3466, and RNA were used in nanomolar concen-

trations in a strict ratio of 1 molecule of GAPDH to 2 of RNA and/or 2 of CGP3466. All samples were dissolved in this buffer. Where indicated, 0.1% of SDS was used. To calibrate the column, the fractions for the following proteins were determined: cytochrome *c* (12.4 kDa) fraction 23, lysozyme (14.4 kDa) fraction 23, carbonic anhydrase (20 kDa) fraction 20, BSA (67 kDa) fraction 18, β-galactosidase (116 kDa) fraction 16, aldolase (158 kDa) fraction 13, and macroglobulin (170 kDa) fraction 10 (see calibration bar below Fig. 7B3). Protein was detected by monitoring the absorbance of individual fractions at 280 nm and confirmed at 293 nm. Nucleic acid was detected similarly by monitoring absorbance at 260 nm.

Results

We previously showed that apoptosis initiated by serum and NGF withdrawal from PND-PC12 cells can be reduced by DEP (Tatton et al., 1994; Wadia et al., 1998). In this study, we used the same model to compare the antiapoptotic capacities of DEP, DES, and CGP3466. Reductions in apoptosis were estimated by two complementary measures: 1) counts of intact nuclei as an indicator of cell survival and 2) counts of cells with nuclear chromatin condensation using a fluorescent DNA binding dye, YOYO-1, as a measure of apoptotic nuclear degradation (examples in Fig. 1, B1 and B2). DES and CGP3466 showed similar or superior capacities to DEP to increase survival (Fig. 1A) and to reduce the proportion of nuclei with chromatin condensation (Fig. 1C) over concentration ranges of 10^{-5} to 10^{-13} M. At 10^{-9} M, all three agents at least doubled the proportion of cells that survived for 24 h after NGF and serum withdrawal. In a similar manner, the same concentration reduced the proportion of cells with nuclear chromatin condensation to less than 25% of that found at 12 h after NGF and serum withdrawal.

We also compared the capacity of a BL-CGP3466 (Zimmermann et al., 1998) for details of the fluorescently labeled DES and CGP3466) with that of CGP3466 in reducing apoptosis in the PND-PC12 model (Fig. 1D). Over the concentration range of 10^{-7} to 10^{-11} M, the BL-CGP3466 retained 75 to 80% of the capacity of CGP3466 to increase cell survival.

We then used the BL-CGP3466 with LCSM to follow the entry and localization of BL-CGP3466 in living PND-PC12 cells maintained in an environmentally controlled chamber. The BL-CGP3466 fluorescence revealed reproducible rates of entry and subcellular localization in the cells and displayed classic competition curves for preadded unlabeled CGP3466. Figure 2 provides an example of the competition in which the addition of 10^{-9} M BL-CGP3466 to the chamber resulted in a gradual accumulation of subcellular fluorescence over about 30 min (Fig. 2, top). The subcellular distribution of the BL-CGP3466

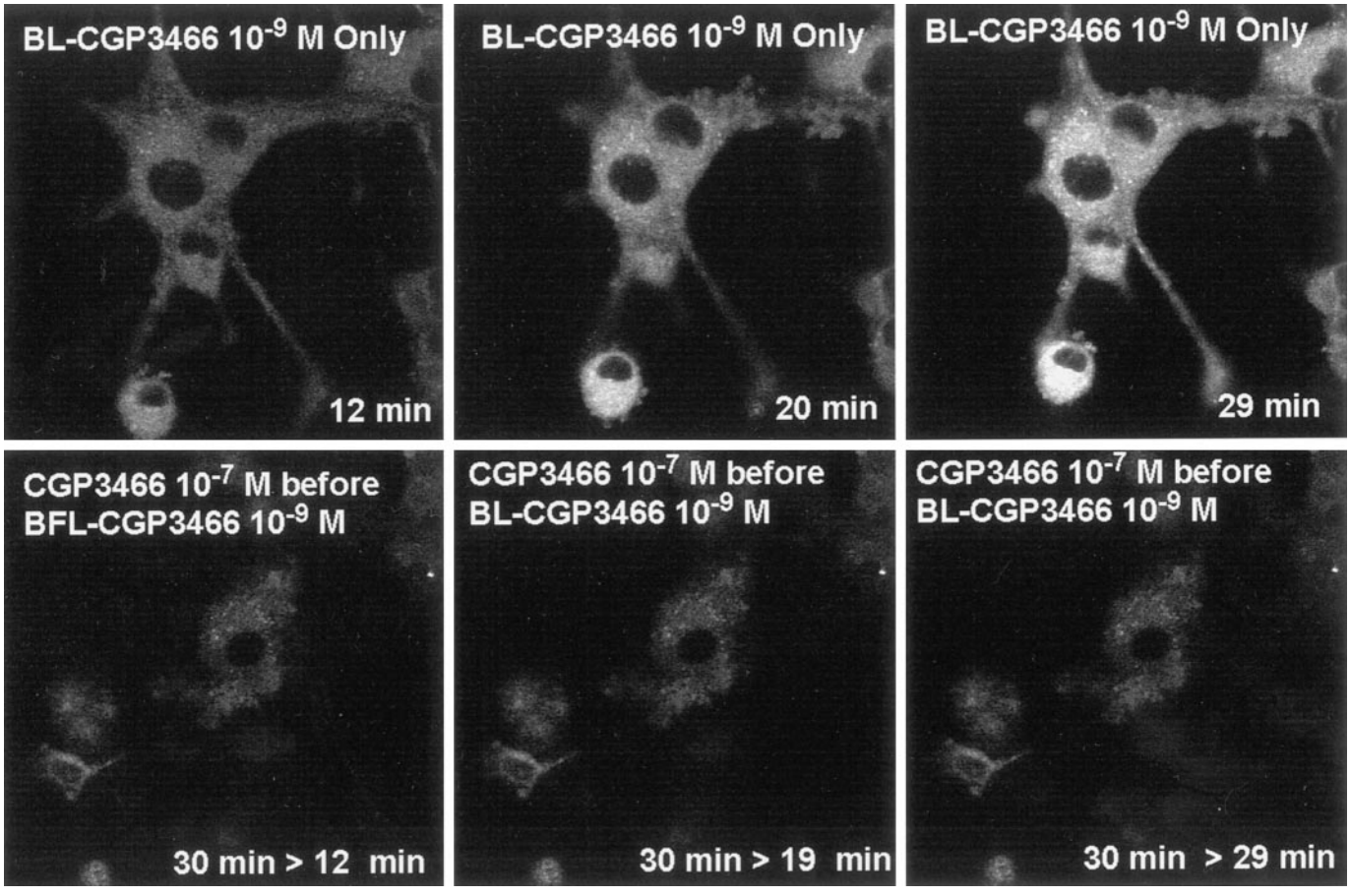

Fig. 2. BL-CGP3466 fluorescence seen with LCSM is gradually retained in the extranuclear cytosol, and preincubation with higher concentrations of unlabeled CGP3466 markedly reduces the retention. Top three panels, LCSM images of the retention of BL-CGP3466 fluorescence in living PND-PC12 cells maintained in an environmental chamber containing MEM with serum and NGF at 12, 20, and 29 min after the addition of 10^{-9} M BL-CGP3466. Note the gradual increase in extranuclear cytosolic fluorescence. Bottom three panels, LCSM images of another group of cells that were preincubated with 10^{-7} M of unlabeled CGP3466 for 30 min before the addition of 10^{-9} M BL-CGP3466 and then imaged at 12, 19, and 29 min. Note that the preincubation with the unlabeled CGP3466 reduced the appearance of the BL-CGP3466 fluorescence at all time points, showing that the BL-CGP3466 retention was specific for CGP3466 binding sites.

fluorescence was very similar to that found for antibodies against GAPDH in the cells (see examples in Fig. 5, A1–A4). That is, the BL-CGP3466 fluorescence gradually accumulated in the extra nuclear cytosol with relatively light and scattered accumulation in the nucleus. Thirty minutes of preincubation of the cells with 10^{-7} M unlabeled CGP3466 followed by the addition of 10^{-9} M BL-CGP3466 markedly reduced the accumulation of BL-CGP3466 fluorescence (Fig. 2, bottom). Similarly, incubation of BL-CGP3466 with paraformaldehyde-fixed PC12 cells on a coverglass showed subcellular distributions of BL-CGP3466 (Fig. 3A1) that were similar, if not identical, to those found in living cells using the environmentally controlled chamber (Fig. 2) and those found for a mouse monoclonal antibody against GAPDH (see Fig. 5A3). Similar results were obtained with BL-DES (not shown).

We used photoaffinity-labeled CGP3466 (Zimmermann et al., 1998) to determine whether the DEP analog binds to GAPDH in the serum and NGF-withdrawn PND-PC12 cells in a similar manner as that reported for rat hippocampal homogenates (Kragten et al., 1998). Autoradiographs revealed major bands at about 37, 43, 50, and possibly 200 kDa, which appeared similar to those found for rat hippocampal tissue. Figure 3B shows a typical autoradiograph for protein extracted from cells at 3, 6, and 9 h after washing and placement in M/O. Figure 3C1 shows a higher power example of the 37-kDa band. The same membranes used for autoradiography were immunoreacted with a monoclonal antibody against GAPDH, and an immunodense band corresponding in position to the 37-kDa autoradiographic band was found (Fig. 3C2 was immunoreacted for the same membrane examined autoradiographically in Fig. 3C1). The similarity of the subcellular distribution of BL-CGP3466 fluorescence and

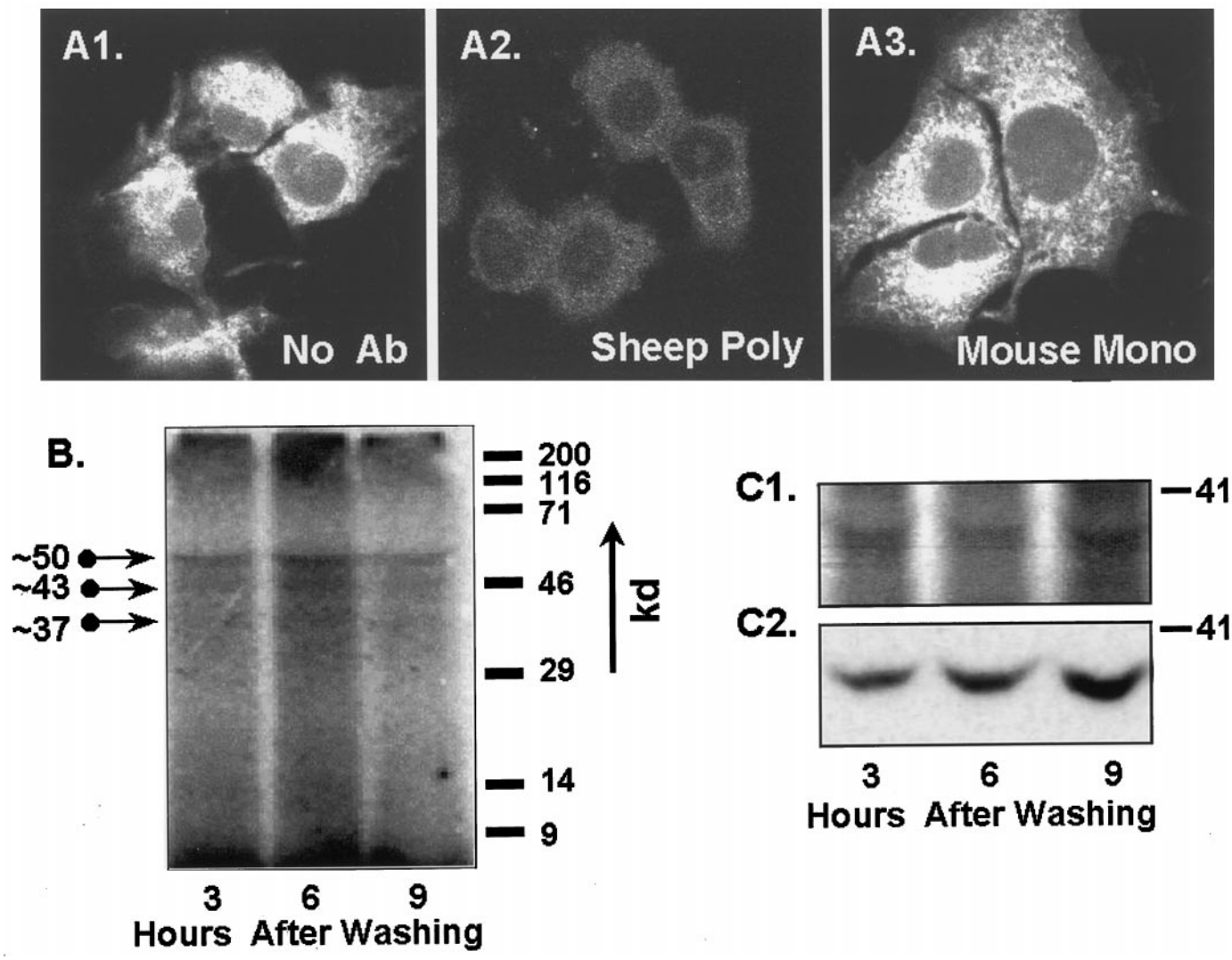

Fig. 3. CGP3466 photoaffinity labeling and BL-CGP3466 labeling of cells imaged with LCSM. A1–A3, paraformaldehyde-fixed cells on coverglass that were incubated with BL-CGP3466 for 30 min and then imaged using LCSM. A2 and A3, cells were preincubated with a sheep polyclonal (1:250) and a mouse monoclonal antibody (1:400) for 30 min before the addition of BL-CGP3466. Note that the BL-CGP3466 fluorescence is scattered throughout the extranuclear cytosol and that the sheep antibody, but not the mouse antibody, blocked the retention of the BL-3466 in the cells. B, autoradiogram for total protein extracted from PND-PC12 cells at 3, 6, and 9 h after serum and NGF withdrawal. Before withdrawal, the cells were incubated with a photoaffinity-labeled, ^{125}I-tagged CGP3466 and then exposed to ultraviolet light to activate the azido group of the photoaffinity label. The autoradiograms revealed at least three bands, as shown, at 37, 43, and 47 kDa. C1, section of a photoaffinity-labeled, ^{125}I-tagged CGP3466 autoradiogram for total protein extracted from PND-PC12 cells at 3, 6, and 9 h after serum and NGF withdrawal showing the distinct band at 37 kDa, which increased in intensity from 3 to 9 h. C2, probing the same membrane with an antibody against GAPDH showed an immunodense band that was located at the identical position to the 37-kDa autoradiography band and also increased in intensity from 3 to 9 h.

GAPDH immunofluorescence and the subcellular colocalization of a portion of photoaffinity-labeled CGP3466 autoradiographic activity with GAPDH immunoreaction seem in accord previous findings showing that one of the proteins binding CGP3466 is GAPDH (Kragten et al., 1998).

In solution, GAPDH can take a monomeric, dimeric, or tetrameric form but greatly favors the tetramer (Minton and Wilf, 1981). Molecular modeling of the GAPDH tetramer revealed a central channel at the interface between the four monomers (see Fig. 7, A1 and A2; also see Fig. 7 in Borden, 1998). Examination of the GAPDH tetramer model suggested that CGP3466 and DES were most likely to bind in this central channel. (See Figure 7B1 for a model of CGP3466 in the channel.) A sheep polyclonal antibody (Biogenesis, Poole, Dorset, UK), which was raised against residues located in a position that would likely block entry to the channel (see location of the residues in Fig. 7C), was applied to fixed cells on a coverglass that were subsequently treated with BL-CGP3466. Cells that were preincubated with the sheep antibody showed markedly reduced BL-CGP3466 cellular fluorescence, even after prolonged incubation with BL-CGP3466 (compare Fig. 3, A1 and A2). In contrast, preincubation with a mouse antibody against GAPDH (Chemicon), which reacted against residues near to the N terminus, placing the residues in or near to the Rossman fold region of the tetramer (see Fig. 7A1, RF), did not alter the BL-CGP3466 fluorescence (compare Fig. 3, A1 and A3).

To determine whether the PND-PC12 cell apoptosis was typical of GAPDH-associated apoptosis found in other cellular models, WESTERN blots were prepared for total protein extracted from cells at multiple time points after washing and placement in medium without serum and NGF. The blots showed that GAPDH levels began to increase at about 2 h after washing and placement in serum and NGF-free medium (Fig. 4A). GAPDH levels did not appear to increase in serum and NGF-withdrawn cells that were treated with 10^{-9} M CGP3466 or 10^{-9} M DES (Fig. 4B).

In parallel experiments, Western blots for protein extracted from the nuclear, mitochondrial, and cytosolic cellular subfractions at 3, 6, 9, and 12 h after serum and NGF withdrawal were examined for GAPDH protein levels. Control blots were prepared for the subfractions using antibodies against nucleolin, cytochrome oxidase, and 14-3-3 β protein that are known to react with proteins in the nuclear, mito-

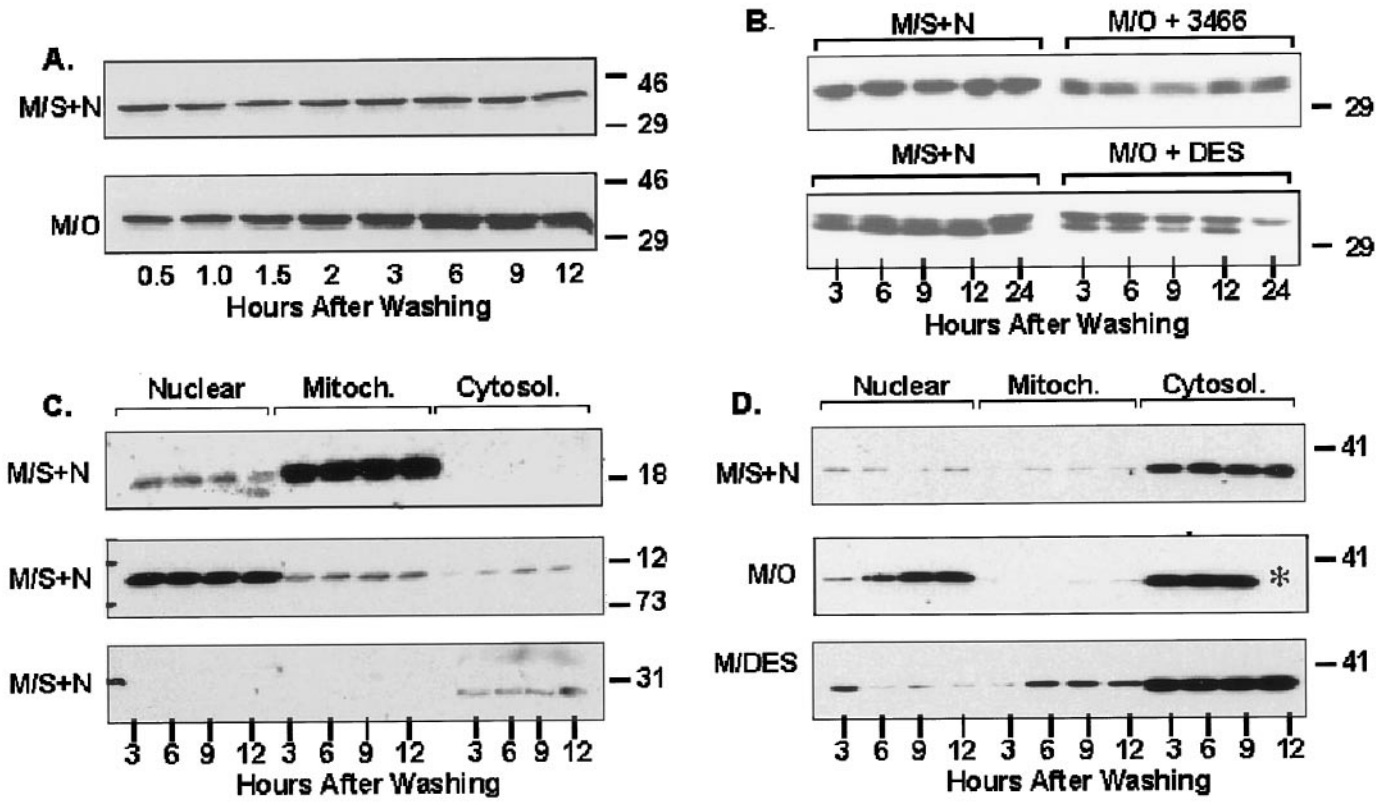

Fig. 4. GAPDH levels increase in PND-PC12 cells after serum and NGF withdrawal, and DES and CGP3466 prevent the increase. A, Western blot labeled M/S+N for an experiment in which cells were washed and replaced in MEM with serum and NGF (top) as a control together with a blot for an experiment in which cells were washed and placed in MEM only (bottom) to induce apoptosis by trophic withdrawal. Note the relative increase in GAPDH immunodensity beginning at the 2-h band after washing for the trophically withdrawn cells but not the control cells. B, similar experiments to those in A but CGP3466 (top) or DES (bottom) at 10^{-9} M was added to the MEM only. Note that the additions prevented increases in GAPDH levels. C, each panel from top to bottom shows immunodensity for the nuclear (Nuclear), mitochondrial (Mitoch.), and cytosolic (Cytosol.) subcellular fractions at 3, 6, 9, and 12 h after washing for nucleolin, cytochrome oxidase, and 14-3-3 β, respectively. Note that each of the protein immunoreactions is concentrated in a different subfraction. D, each panel shows Western blots for protein taken from the subcellular fractions at 3, 6, 9, and 12 h after washing and replacement into MEM with serum and NGF as a control (top) or placement into MEM only to induce apoptosis (middle). Note the progressive increase in nuclear GAPDH beginning between 3 and 6 h after washing and serum and NGF withdrawal together with the maintained increase in cytosolic GAPDH that was present at 3 to 9 h. Similar panels for experiments in which the cells were placed in MEM with 10^{-9} M DES (bottom) after washing. Note that the DES prevents the progressive increase in GAPDH immunoreactivity in the nuclear subfraction. On all blots, identical amounts of total protein were loaded into each lane. *In the 12 h Cytosol. lane for the M/O panel, indicates that protein was not loaded onto that lane.

chondrial, and cytosolic fractions, respectively (see Fig. 4C for examples of the use of the three antibodies with protein subfractions taken from cells in M/S+N). The blots indicated that GAPDH was largely concentrated in the cytosolic subfraction in control cells that were washed and then replaced into M/S+N. GAPDH levels appeared to increase in the cytosolic subfraction after serum and NGF withdrawal and also progressively increased in the nuclear subfraction at each of the 3-, 6-, 9-, and 12-h time points. Treatment with 10^{-9} M DES or CGP3466 largely prevented the increase in GAPDH immunoreaction for the nuclear fraction.

Recognizing that subcellular fractionation enriches the proportions of proteins localized in particular organelles but may not exclusively contain proteins from those organelles (see Fig. 4C), we also examined the subcellular distribution of GAPDH immunoreactivity using LCSM. The GAPDH immunocytochemistry combined with YOYO-1 staining for DNA showed that GAPDH was concentrated in the cytosol with only light punctate immunoreaction in the nuclei in control cells that were washed and then replaced in M/S+N (see examples in Fig. 5, A1–A4). Serum and NGF withdrawal induced a dense increase in nuclear GAPDH immunoreaction, excluding the nucleolus (see examples in Fig. 5, B1–B4). The nuclear increase and subnuclear distribution were similar to those we demonstrated using a GAPDH-green fluorescent fusion protein in several other models of apoptosis (Shashidharan et al., 1999).

During the first 24 h after washing and replacement into medium with serum and NGF, about 2 to 3% of control cells showed baseline dense nuclear GAPDH immunoreactivity at all time points (Fig. 6C2), contrasting with those that were NGF and serum withdrawn, in which about 6% showed dense nuclear GAPDH immunoreactivity by 3 h, followed by a progressive increase to about 25% by 12 h. On average, the increase in nuclei with dense nuclear GAPDH immunoreaction preceded the increase in nuclei with chromatin condensation, as demonstrated by YOYO-1 staining by at least 3 h (compare Fig. 6, C1 and C2). Treatment with 10^{-9} M DES or CGP3466 markedly reduced both the percentage of nuclei with chromatin condensation and those with dense GAPDH immunoreaction at all time points (Fig. 6, B1 and B2). Accordingly, Western blotting and LCSM immunocytochemistry indicated that both DES and CGP3466 reduce the increased levels of GAPDH and the nuclear accumulation of GAPDH that occurs early in apoptosis induced in PND-PC12 cells by serum and NGF withdrawal.

In an attempt to understand the basis for DES and CGP3466 prevention of increases in GAPDH levels and GAPDH nuclear accumulation, we first examined the effect of CGP3466 and DES on the glycolytic activity of GAPDH in vitro. The addition of 10^{-9} M CGP3466 to GAPDH in solution by itself did not alter the extent or rate of NAD^+ conversion to NADH (Fig. 6A1). The Rossman fold region of GAPDH binds tRNA and AU-rich RNA, particularly AUUUA base sequences ((Nagy and Rigby, 1995; also see a computer model of RNA binding in the Rossman fold in Fig. 6 of Borden, 1998). We therefore added a synthetic RNA with repeated AUUUA sequences to the solution and found that the addition reduced the extent of NADH production by about 25% (Fig. 6A1). The addition of CGP3466 to the solution containing both GAPDH and the synthetic RNA resulted in almost complete recovery of the NADH production. Similar results were obtained with DES (not shown).

We then examined the conversion of NAD^+ to NADH in cell lysates after washing (Fig. 6A2). We chose a 6-h time point because GAPDH levels were markedly increased (Fig. 4A) but relatively few cells had entered the phase of nuclear degradation at that time (Fig. 5C1). Lysates from cells that had undergone serum and NGF withdrawal showed marked increases in both the extent and rate of NAD^+ to NADH conversion compared with control cells in M/S+N. The addition of 10^{-9} M DES to the withdrawn cells induced a partial reduction in the extent of NAD^+ to NADH conversion. Accordingly, these data suggest that the addition of DEP-like compounds can alter GAPDH glycolytic activity, possibly by altering the configuration of GAPDH or its interaction with AU-rich RNA.

Because binding of CGP3466 in the channel of tetrameric GAPDH might alter the interface between the substituent GAPDH monomers (Fig. 7A2), we used size exclusion chromatography to determine whether CGP3466 or DES affected the oligomeric form of the enzyme. The addition of 10^{-9} M CGP3466 (or DES) to GAPDH in solution altered a major proportion of the protein from a size equivalence of 148 kDa to 74 kDa (Fig. 6B1, see size exclusion calibration scale below Fig. 6B3), consistent with a change from a tetrameric form to a dimeric form. Similarly, the addition of poly(U) RNA to GAPDH in solution shifted the peak to a size equivalence of more than 200 kDa, and the addition of CGP3466 (or DES) induced size equivalence changes indicative of the freeing of tetrameric GAPDH from the RNA and its conversion to a dimeric form (Fig. 6B2). GAPDH was placed in SDS to convert it to a monomer. The addition of CGP3466 or DES to the solution containing SDS induced a shift in the size equivalence of the major peak, suggesting a change in the configuration of the monomeric form, and converted a small proportion of the protein to a size equivalence consistent with a dimer (Fig. 6B3).

Discussion

The serum and NGF-withdrawn PND-PC12 cells showed increases in GAPDH levels and nuclear GAPDH accumulation that were similar to those reported for other apoptosis models (Sunaga et al., 1995; Ishitani et al., 1996, 1997, 1998; Saunders et al., 1997; Sawa et al., 1997; Shashidharan et al., 1999). Most importantly, CGP3466 and DES prevented both the increases in GAPDH and the nuclear accumulation. Transcriptional or translational inhibitors can reduce the increase in GAPDH levels in early apoptosis (Ishitani et al., 1997), suggesting that newly synthesized GAPDH contributes to the protein's role in apoptosis. The signaling pathways that lead to increased GAPDH levels in early apoptosis are not known. p53 overexpression induces apoptosis that is associated with downstream increases in expression of a large number of genes, including GAPDH (Polyak et al., 1997). Accordingly, a p53-dependent signaling pathway may contribute to GAPDH-associated apoptosis. Our recent studies using the expression of GAPDH/green fluorescent fusion protein have shown accumulation of the fusion protein in the nuclei of a variety of cell types in early apoptosis (Shashidharan et al., 1999). The accumulation of the fusion protein was similar to that shown in the serum and NGF-withdrawn PND-PC12 cells in the present study and pro-

vided evidence that at least part of the GAPDH that accumulates in the nucleus was previously resident in the cytoplasm and was not newly synthesized.

This study, similar to our previous studies (Tatton et al., 1994; Wadia et al., 1998), showed that apoptotic nuclear degradation begins in the PND-PC12 cells at about 6 h after serum and NGF withdrawal and is maximal at 12 to 18 h. Therefore, the increases in GAPDH levels and GAPDH nuclear accumulation are early events in this form of apoptosis and precedes the onset of nuclear degradation by 3 or more hours. Hence, the participation of GAPDH in the apoptotic cascade seems to be well upstream from the events that mediate apoptotic degradation.

DES is a relatively poor MAO-B inhibitor compared with DEP (Heinonen et al., 1997), and CGP3466 does not inhibit MAO-B (Kragten et al., 1998). Decreases in apoptosis with

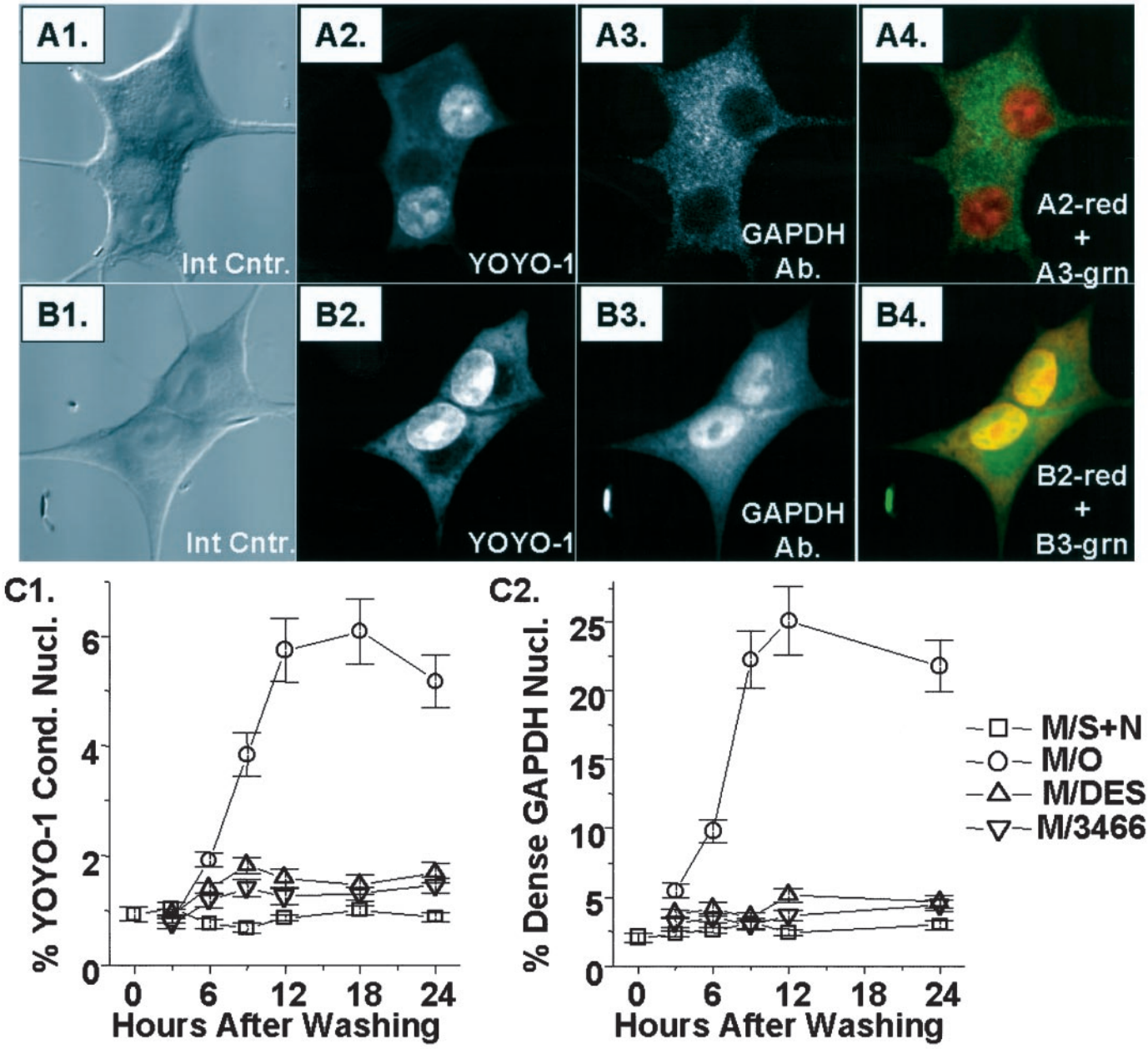

Fig. 5. GAPDH immunoreactivity in PND-PC12 cells after serum and NGF withdrawal visualized with LCSM. A1–A4, LCSM micrographs from identical image fields consist of an interference contrast micrograph, fluorescence micrograph for YOYO-1 DNA binding, immunoctrochemistry for GAPDH, and a combined image in which A2 (recolored red) and A3 (recolored green) were digitally added. The cells were washed and then replaced in MS+N as a control (example at 6 h after washing). The maintained separation of the red and green color in A4 shows that GAPDH is largely extranuclear in location. B1–B4, an identical series of LCSM micrographs for cells that were washed and placed in MO to induce apoptosis by serum and NGF withdrawal showed dense GAPDH immunoreaction in the nucleus that spared the nucleolus (example at 6 h after washing). The orange-yellow color in B4 shows the colocalization of DNA YOYO-1 binding and GAPDH immunoreaction and illustrates typical dense nuclear GAPDH accumulation. C1 and C2, counts of cells with nuclei showing YOYO-1-stained chromatin condensation, and those with dense GAPDH nuclear immunoreaction, respectively, show that the percentages of nuclei with GAPDH nuclear accumulation was significantly increased by 3 h after washing, whereas the percentages with apoptotic chromatin condensation did not begin to increase until 6 h after washing and placement in MEM only. DES (plots labeled M/DES) and CGP3466 (plots labeled M/3466) at 10^{-9} M markedly decreased the percentage of nuclei with chromatin condensation and those with dense GAPDH nuclear immunoreaction.

DEP or DES can be obtained at concentrations or dosages that do not inhibit MAO-A or MAO-B (Ansari et al., 1993; Tatton and Chalmers-Redman, 1996; Le et al., 1997). In this study, concentrations of DEP and DES ranging from 10^{-5} to 10^{-13} M showed similar capacities to increase survival, whereas CGP3466 induced greater levels of survival, particularly at concentrations of less than 10^{-9} M. Cytochrome P-450 inhibitors block the capacity of DEP, but not DES, to reduce apoptosis in a variety of apoptosis models (W. G. Tatton and R. M. Chalmers-Redman, unpublished observations). Accordingly, the antiapoptotic capacity of DEP appears to depend on its metabolism to DES.

Based on our results with photoaffinity CGP3466 and the BL-labeled compounds, it is likely that CGP3466 and DES bind to GAPDH in the PND-PC12 cells in a similar manner to that shown for rat hippocampus (Kragten et al., 1998). Our antibody studies suggest that the binding may occur in or near to the channel of GAPDH tetramer. Size exclusion data indicate that a portion of GAPDH converts to a dimer in the presence of CGP3466 or DES. There are three possible dimers that could be produced (Fig. 7, D1–D3): 1) the channel could be bisected lengthwise, resulting in a loss of the channel but retaining the RNA binding site in the Rossman fold; 2) the channel is bisected across its width, resulting in a dimer with a channel but no RNA binding site; and 3) the channel is cut across its width so that two diagonally associated monomers form the dimer. At this time, we do not have data to predict which of these dimer forms predominate. DEP that has not been metabolized to DES may not bind to GAPDH. Studies using photoaffinity-labeled DEP in the presence of cytochrome P-450 inhibitors will be required to determine whether DEP itself can bind to GAPDH.

CGP3466 differs from DES in the replacement of the single phenol ring with three rings, the center of which includes an oxygen. In BL-CGP3466 and BL-DES, the BODIPY was attached to the ring portions of the compounds through a flexible link (Zimmermann et al., 1998). We showed that both BL compounds retain most of their capacity to reduce apoptosis in the serum and NGF-withdrawn PND PC12 cells. Furthermore, even with the attachment of the relatively bulky BODIPY moiety, BL-CGP3466 accumulated in the cells with a subcellular distribution similar to those found for GAPDH immunoreactivity. Our modeling suggests that the bulky BODIPY moiety should not interfere with binding in the channel. BL-CGP3466 entry to the subcellular sites could be blocked by preincubation with higher concentrations of

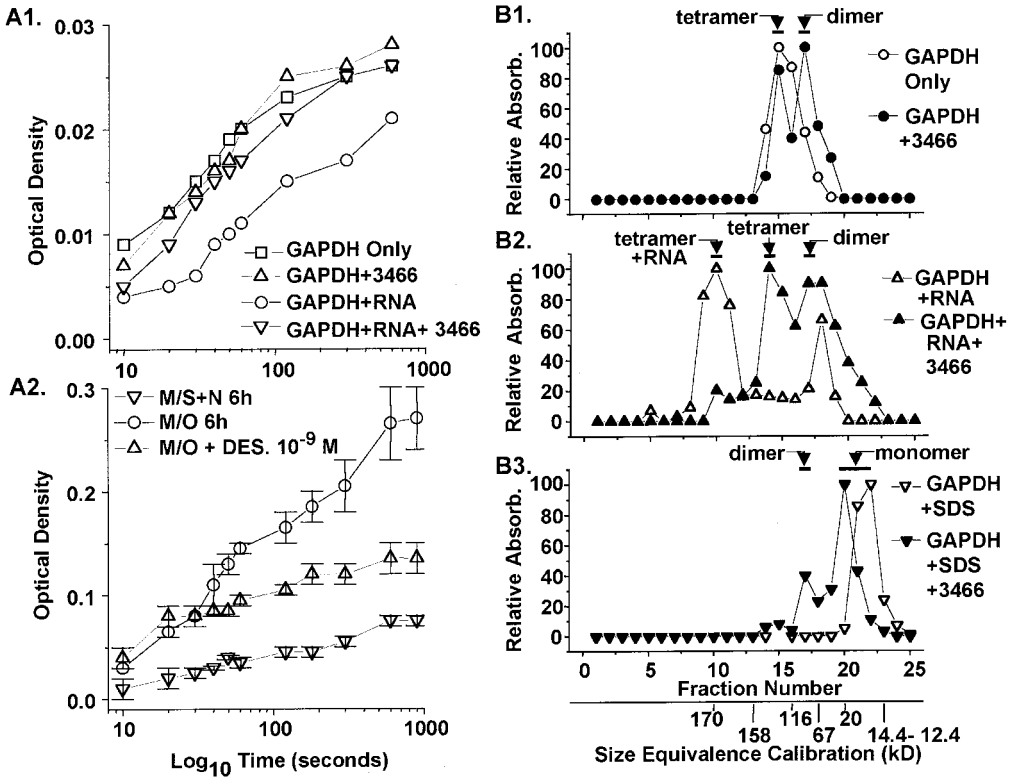

Fig. 6. Effects of CGP3466 on the glycolytic capacity of GAPDH in vitro and in vivo and evidence for the conversion of GAPDH to a dimer by CGP3466. A1, NADH production from NAD^+ over time was measured in an in vitro system. The addition of CGP3466 does not significantly alter enzymatic activity of GAPDH, whereas the addition of AUUUA synthetic RNA sequences had little effect on the rate but reduced extent of the glycolytic activity of GAPDH. The addition of 10^{-9} M CGP3466 induced a recovery of glycolytic activity, suggesting that the compound altered the relationship between GAPDH and RNA. A2, measurement of NAD^+ to NADH conversion in lysates taken at 6 h after washing from control cells (M/S+N 6 h), cells after NGF and serum withdrawal (M/O 6 h)m and cells after serum and NGF withdrawal treated with 10^{-9} M DES (M/O+DES 6 h). B1–B3, size exclusion chromatography for GAPDH in solution alone, with poly(U) RNA, or with detergent. B1. GAPDH alone in solution forms a tetramer with a size equivalence of 148 kDa in fraction 14. In the presence of 10^{-9} M CGP3466, more than half of GAPDH appears as a dimer in fraction 17 with a size equivalence of 74 kDa. B2, GAPDH binds to poly(U) RNA. The peak at fraction 10, which indicates a size equivalence of more than 170 kDa, indicates an amalgam of RNA and GAPDH. Fraction 10 was also shown to include RNA by the finding of a peak at 260 nm on the spectrophotometer. In the presence of 10^{-9} M CGP3466, the shifts in the equivalence values of the peaks indicate that GAPDH has separated from RNA and that there is a large increase in GAPDH dimer. B3, in the presence of 0.1% SDS, GAPDH alone is found in fraction 23 with a size equivalence consistent with a monomer. After the addition of 10^{-9} M CGP3466, a small proportion of GAPDH shows a size equivalence consistent with a dimer, even in the presence of the detergent.

unlabeled CGP3466, which indicated the specificity of the BL compounds for CGP3466 binding sites. This is the first report of the use of a fluorescently labeled compound with LCSM to examine the subcellular localization and the binding specificity of a compound in living or fixed cells.

GAPDH largely exists as a tetramer with minor populations of dimers and monomers. Our data indicate that CGP3466 and DES increase the stability of GAPDH as a dimer. We therefore propose that agents that stabilize GAPDH as a dimer, rather than a tetramer, prevent the early apoptotic GAPDH increase and nuclear accumulation and thereby induces a decrease in apoptosis. If GAPDH dimer cannot accumulate in the nucleus, it would explain part of our results. It is more difficult to understand how the presence of GAPDH dimer would prevent GAPDH up-regulation. The increased expression may depend on nuclear accumulation of constitutive protein. Our findings indicating a tetrameric/dimeric conversion were obtained in vitro, and it is therefore possible that GAPDH dimerization does not occur in vivo in response to DES or CGP3466 binding. In vivo, the binding of the DEP-related compounds to GAPDH might result in a more subtle change in GAPDH structure. If, as we have hypothesized, the conversion of GAPDH to a dimer robs the protein of its capacity to participate in apoptosis, the DEP-related compounds will be the first compounds shown to reduce cell death by altering oligomerization.

In vitro, the DEP-like compound binding results in stabilization of the dimer, increases the catalysis of glycolytic activity by GAPDH, and decreases GAPDH affinity for RNA. These effects are likely interrelated. The glycolytic action and RNA binding of GAPDH occur in the same region of the protein. Conversion of GAPDH from a tetramer to a dimer is known to increase its glycolytic capacity (Minton and Wilf, 1981). Dimerization of GAPDH, together with a freeing of GAPDH from AUUUA RNA, could explain the facilitation of glycolysis by CGP3466 and DES in vitro.

This is the first study to show increased glycolytic activity in cells entering apoptosis. The increase may result from the increase in GAPDH levels associated with apoptosis in the PND-PC12 cells. It also could result, in part, from freeing of the Rossman fold region of the protein from AUUUA-rich RNA binding with consequent increased availability of the fold for NAD^+ to NADH conversion. The relative decrease in glycolysis induced by the DEP-like compounds likely reflects their capacity to reduce or prevent the increase in GAPDH levels that we found in early apoptosis.

The DEP-related compounds appear to reduce the apoptotic function of GAPDH while at the same time facilitating or maintaining the glycolytic function of protein at levels that exceed those in control cells but are reduced compared with those in apoptotic cells. GAPDH is a multifunction protein and participates in functions like tubulin polymerization, endocytosis, translational control of gene expression, nuclear tRNA export, DNA replication, and DNA repair (see Sirover,

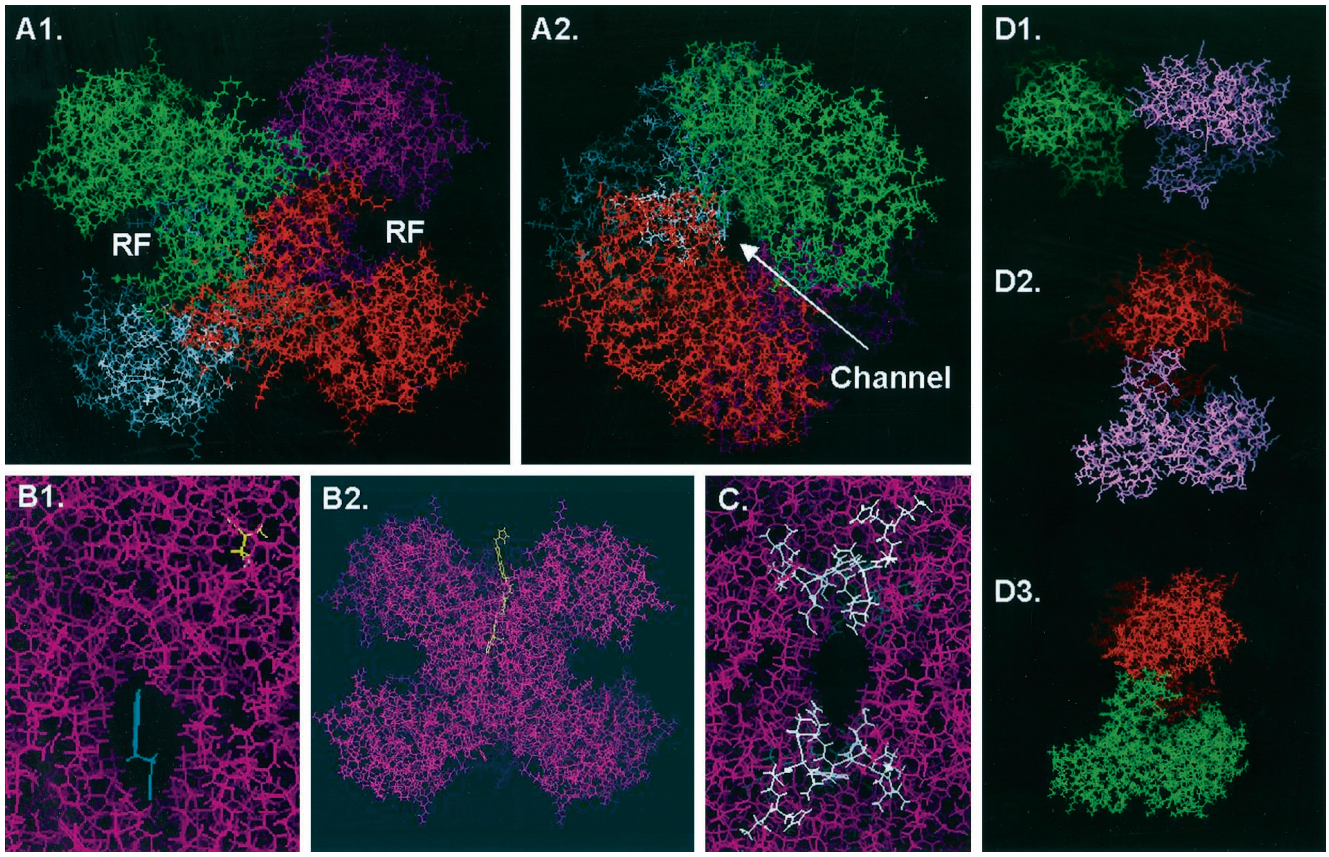

Fig. 7. Models of the rat GAPDH tetramer showing the putative DEP-like compound binding channel. A1, the four identical monomers which make up the GAPDH tetramer are shown in different colors. The NAD^+ binding site, the Rossmann fold, is indicated by RF. A2, a 90-degree rotation of the image in A1. The putative DEP-like compound binding channel is indicated where the four monomers join. B1, CGP3466 (blue) is shown in the channel. B2, a view of CGP3466-BODIPY (yellow) located in the channel. C, residues in white indicate the epitope site for the sheep polyclonal antibody, which reduced the cellular accumulation of BL-CGP3466. D1–D3, the three possible dimers of GAPDH that might be formed by the binding of DEP-like compounds. All images were produced in Insight (Biosym).

1997). It will be interesting to determine which of those functions are maintained and which are altered by the binding of DEP-related compounds.

In normal nuclei, GAPDH binds to promyelocytic leukemia (PML) protein in an RNA-dependent fashion (Carlile et al., 1998). PML localizes to PML nuclear bodies, which have been implicated in apoptosis, suppression of oncogenic transformation and growth suppression (Melnick and Licht, 1999). PML and the other protein components of PML nuclear bodies appear to function in regulation of both transcription and translation (Borden et al., 1998). Nuclear GAPDH could therefore contribute to apoptosis by modifying either transcription (Ronai, 1993) or translation (Sioud and Jespersen, 1996), perhaps mediated through an interaction with PML.

Finally, DEP-related compounds have been shown to reduce neuronal and non-neuronal death in a wide variety of models, many of which are independent of MAO-B inhibition (Tatton and Chalmers-Redman, 1996). The basis for clinical slowing of the progression of PD (Parkinson's Study Group, 1993; Olanow et al., 1995) and the preliminary indications of improvement in HD with DEP treatment (Patel et al., 1996) are unknown and have been variously suggested to result from slowed neuronal death (Olanow et al., 1995), improved dopaminergic transmission or increased dopamine levels (Schulzer et al., 1992), and the actions of the DEP metabolites (−)-amphetamine and (−)-methamphetamine (Karoum et al., 1982). If GAPDH contributes to a reduction in neuronal death in PD, the clinical benefits of DEP treatment may result, in part, from the action of DES on GAPDH rather than on MAO-B.

Acknowledgments

CGP3466, photoaffinity-labeled CGP3466, BL-CGP3466, and BL-DES were provided by Novartis (Basel, Switzerland). Dr. J. Casals contributed to the preparation of the manuscript.

References

Ansari KS, Yu PH, Kruck TP and Tatton WG. (1993) Rescue of axotomized immature rat facial motoneurons by R(−)-deprenyl: Stereospecificity and independence from monoamine oxidase inhibition. *J Neurosci* **13:**4042–4053.

Borden KL (1998) Structure/function in neuroprotection and apoptosis. *Ann Neurol* **44:**S65–S71.

Borden KL, Campbell Dwyer EJ, Carlile GW, Djavani M and Salvato MS (1998) Two ring finger proteins, the ocoprotein PMB and the arenavirus protein Z associate with the ribosomal P-proteins. *J Virol* **72:**3819–3826.

Burke JR, Enghild JJ, Martin ME, Jou YS, Myers RM, Roses AD, Vance JM and Strittmatter WJ (1996) Huntington and DRPLA proteins selectively interact with the enzyme GAPDH. *Nat Med* **2:**347–350.

Carlile GW, Tatton WG and Borden KLB (1998) Demonstration of a RNA-dependent nuclear interaction between the promelocytic leukaemia protein and glyceraldehyde-3-phosphate dehydrogenase. *Biochem J* **335:**691–696.

Cotman CW (1998) Apoptosis decision cascades and neuronal degeneration in Alzheimer's disease. *Neurobiol Aging* **19:**S29–S32.

Fahn S (1996) Controversies in the therapy of Parkinson's disease. *Adv Neurol* **69:**477–486.

Heinonen EH, Anttila MI, Karnani HL, Nyman LM, Vuorinen JA, Pyykko KA and Lammintausta RA (1997) Desmethylselegiline, a metabolite of selegiline, is an irreversible inhibitor of monoamine oxidase type B in humans. *J Clin Pharmacol* **37:**602–509.

Ishitani R, Sunaga K, Hirano A, Saunders P, Katsube N and Chuang DM (1996) Evidence that glyceraldehyde-3-phosphate dehydrogenase is involved in age-induced apoptosis in mature cerebellar neurons in culture. *J Neurochem* **66:**928–935.

Ishitani R, Sunaga K, Tanaka M, Aishita H and Chuang DM (1997) Overexpression of glyceraldehyde-3-phosphate dehydrogenase is involved in low K^+-induced apoptosis but not necrosis of cultured cerebellar granule cells. *Mol Pharmacol* **51:**542–550.

Ishitani R, Tanaka M, Sunaga K, Katsube N and Chuang DM (1998) Nuclear localization of overexpressed glyceraldehyde-3-phosphate dehydrogenase in cultured cerebellar neurons undergoing apoptosis. *Mol Pharmacol* **53:**701–707.

Karoum F, Chuang LW, Eisler T, Calne DB, Liebowitz MR, Quitkin FM, Klein DF and Wyatt RJ (1982) Metabolism of (−) deprenyl to amphetamine and methamphetamine may be responsible for deprenyl's therapeutic benefit: A biochemical assessment. *Neurology* **32:**503–509.

Kim H, Feil IK, Verlinde CL, Petra PH and Hol WG (1995) Crystal structure of glycosomal glyceraldehyde-3-phosphate dehydrogenase from *Leishmania mexicana*: Implications for structure-based drug design and a new position for the inorganic phosphate binding site. *Biochemistry* **34:**14975–14986.

Kish SJ, Lopes-Cendes I, Guttman M, Furukawa Y, Pandolfo M, Rouleau GA, Ross BM, Nance M, Schut L, Ang L and DiStefano L (1998) Brain glyceraldehyde-3-phosphate dehydrogenase activity in human trinucleotide repeat disorders. *Arch Neurol* **55:**1299–1304.

Kragten E, Lalande I, Zimmermann K, Roggo S, Schindler P, Muller D, van Oostrum J, Waldmeier P and Furst P (1998) Glyceraldehyde-3-phosphate dehydrogenase, the putative target of the antiapoptotic compounds CGP 3466 and R-(−)-deprenyl. *J Biol Chem* **273:**5821–5828.

Le W, Jankovic J, Xie W, Kong R and Appel SH (1997) (−)-Deprenyl protection of 1-methyl-4 phenylpyridium ion (MPP+)-induced apoptosis independent of MAO-B inhibition. *Neurosci Lett* **224:**197–200.

Magyar K, Szende B, Lengyel J, Tarczali J and Szatmary I (1998) The neuroprotective and neuronal rescue effects of (−)-deprenyl. *J Neural Transm Suppl* **52:**109–123.

Maruyama W, Takahashi T and Naoi M (1998) (−)-Deprenyl protects human dopaminergic neuroblastoma SH-SY5Y cells from apoptosis induced by peroxynitrite and nitric oxide. *J Neurochem* **70:**2510–2515.

Melnick A and Licht JD (1999) Deconstructing a disease: RARalpha, its fusion partners, and their roles in the pathogenesis of acute promyelocytic leukemia. *Blood* **93:**3167–3215.

Minton AP and Wilf J (1981) Effect of macromolecular crowding upon the structure and function of an enzyme: Glyceraldehyde-3-phosphate dehydrogenase. *Biochemistry* **20:**4821–4826.

Nagy E and Rigby WF (1995) Glyceraldehyde-3-phosphate dehydrogenase selectively binds AU-rich RNA in the NAD(+)-binding region (Rossmann fold). *J Biol Chem* **270:**2755–2763.

Olanow CW, Hauser RA, Gauger L, Malapira T, Koller W, Hubble J, Bushenbark K, Lilienfeld D and Esterlitz J (1995) The effect of deprenyl and levodopa on the progression of Parkinson's disease. *Ann Neurol* **38:**771–777.

Parkinson's Study Group (1993) Effects of tocopherol and deprenyl on the progression of disability in early Parkinson's disease. *N Engl J Med* **328:**176–183.

Patel SV, Tariot PN and Asnis J (1996) L-Deprenyl augmentation of fluoxetine in a patient with Huntington's disease. *Ann Clin Psychiatry* **8:**23–26.

Paterson IA, Barber AJ, Gelowitz DL and Voll C (1997) (−)Deprenyl reduces delayed neuronal death of hippocampal pyramidal cells. *Neurosci Biobehav Rev* **21:**181–186.

Paterson IA, Zhang D, Warrington RC and Boulton AA (1998) *R*-Deprenyl and *R*-2-heptyl-N-methylpropargylamine prevent apoptosis in cerebellar granule neurons induced by cytosine arabinoside but not low extracellular potassium. *J Neurochem* **70:**515–523.

Petersen A, Mani K and Brundin P (1999) Recent advances on the pathogenesis of Huntington's disease. *Exp Neurol* **157:**1–18.

Polyak K, Xia Y, Zweier JL, Kinzler KW and Vogelstein B (1997) A model for p53-induced apoptosis [see comments]. *Nature (Lond)* **389:**300–305.

Ronai Z (1993) Glycolytic enzymes as DNA binding proteins. *Int J Biochem* **25:**1073–1076.

Saunders PA, Chalecka-Franaszek E and Chuang DM (1997) Subcellular distribution of glyceraldehyde-3-phosphate dehydrogenase in cerebellar granule cells undergoing cytosine arabinoside-induced apoptosis. *J Neurochem* **69:**1820–1828.

Sawa A, Khan AA, Hester LD and Snyder SH (1997) Glyceraldehyde-3-phosphate dehydrogenase: Nuclear translocation participates in neuronal and nonneuronal cell death. *Proc Nat Acad Sci USA* **94:**11669–11674.

Schulzer M, Mak E and Calne DB (1992) The antiparkinson efficacy of deprenyl derives from transient improvement that is likely to be symptomatic [see comments]. *Ann Neurol* **32:**795–798.

Shashidharan P, Chalmers-Redman RM, Carlile GW, Rodic V, Gurvich N, Yuen T, Tatton WG and Sealfon SC (1999) Nuclear translocation of GAPDH-GFP fusion protein during apoptosis. *Neuroreport* **10:**1149–1153.

Sioud M and Jespersen L (1996) Enhancement of hammerhead ribozyme catalysis by glyceraldehyde-3- phosphate dehydrogenase. *J Mol Biol* **257:**775–789.

Sirover MA (1997) Role of the glycolytic protein, glyceraldehyde-3-phosphate dehydrogenase, in normal cell function and in cell pathology. *J Cell Biochem* **66:**133–140.

Sunaga K, Takahashi H, Chuang DM and Ishitani R (1995) Glyceraldehyde-3-phosphate dehydrogenase is over-expressed during apoptotic death of neuronal cultures and is recognized by a monoclonal antibody against amyloid plaques from Alzheimer's brain. *Neurosci Lett* **200:**133–136.

Tatton NA, Maclean-Fraser A, Tatton WG, Perl DP and Olanow CW (1998) A fluorescent double-labeling method to detect and confirm apoptotic nuclei in Parkinson's disease. *Ann Neurol* **44:**S142–S148.

Tatton WG and Chalmers-Redman RM (1996) Modulation of gene expression rather than monoamine oxidase inhibition: (−)-Deprenyl-related compounds in controling neurodegeneration. *Neurology* **47:**S171–S183.

Tatton WG, Ju WY, Holland DP, Tai C and Kwan M (1994) (−)-Deprenyl reduces PC12 cell apoptosis by inducing new protein synthesis. *J Neurochem* **63:**1572–1575.

Wadia JS, Chalmers-Redman RME, Ju WJH, Carlile GW, Phillips JL, Fraser AD and Tatton WG (1998) Mitochondrial membrane potential and nuclear changes in apoptosis caused by serum and nerve growth factor withdrawal: Time course and modification by (−)-deprenyl. *J Neurosci* **18:**932–947.

Zimmermann K, Roggo S, Kragten E, Furst P and Waldmeier P (1998) Synthesis of tools for target identification of the anti-apoptotic compound CGP 3466: Part I. *Bioorg Med Chem Let* **8:**1195–1200.

Send reprint requests to: Dr. William G. Tatton, Department of Neurology, Annenberg 14-70, Mount Sinai Medical Center, One Gustave L. Levy Place, New York, NY 10029. E-mail: william_tatton@smtplink.mssm.edu